

# [Ni(en)<sub>3</sub>][InSbS<sub>4</sub>]: A One-Dimensional Polymeric Indium Thioantimonate with a Polar Structure

Mei-Ling Feng,<sup>[a]</sup> Pei-Xin Li,<sup>[a]</sup> Ke-Zhao Du,<sup>[a]</sup> and Xiao-Ying Huang\*<sup>[a]</sup>

*Dedicated to Professor John D. Corbett on the occasion of his 85th birthday*

**Keywords:** Indium / Antimony / Sulfur / Non-centrosymmetric compounds / Structure elucidation

A polar indium thioantimonate, namely [Ni(en)<sub>3</sub>][InSbS<sub>4</sub>] (**1**) (en = ethylenediamine), has been synthesized under solvothermal conditions. Its structure features a left-handed helical anionic chain of [InSbS<sub>4</sub>]<sub>n</sub><sup>2n−</sup> moieties built upon trinuclear heterometallic clusters of {In<sub>2</sub>SbS<sub>8</sub>} as secondary building units. The [Ni(en)<sub>3</sub>]<sup>2+</sup> cations, acting as structure directors

and charge balancing agents, are located among the chains and form extensive N–H⋯S and C–H⋯S hydrogen bonds with the S atoms of the anionic chains. The thermal stability, optical and ferroelectric properties, as well as theoretical band structure and density of states (DOS) have been studied.

## Introduction

Crystallographically non-centrosymmetric (NCS) compounds can exhibit interesting physical properties such as ferroelectricity, piezoelectricity, pyroelectricity, and second-order nonlinear optical (NLO) activity and can further have potential applications in the fields of electronic and optics.<sup>[1,2]</sup> The rational design and preparation of NCS compounds are challenging because most compounds show a tendency to crystallize in a centrosymmetric space group. An effective strategy for inducing the NCS compound is to introduce non-centrosymmetrical or chiral building units into the structure. Such units include distorted polyhedra with a d<sup>0</sup> transition-metal cation center, non-centrosymmetric polyhedra adopted by the main group cations with stereochemically active lone-pair electrons (such as Se<sup>4+</sup>, Te<sup>4+</sup>, As<sup>3+</sup>, Sb<sup>3+</sup>), chiral organic molecules, chiral metal complexes, amongst others.<sup>[2–4]</sup> Further, NCS compounds combining two kinds of non-centrosymmetrical structural building units have been reported. For example, the combination of a d<sup>0</sup> transition-metal cation and a main group cation possessing stereochemically active lone-pair electrons in one structure has resulted in some NCS oxides with excellent NLO properties.<sup>[3,5]</sup>

NCS chalcogenide materials have promising applications in the fields of NLO in the IR region and information stor-

age.<sup>[6]</sup> The M<sup>3+</sup> cations of group 15 (M = As, Sb) tend to form non-centrosymmetric coordination polyhedra with chalcogenide ligands.<sup>[7]</sup> NCS chalcogenides based on such non-centrosymmetric structural building units have been realized, some of which exhibit strong nonlinear optical responses.<sup>[8]</sup> On the other hand, studies indicate that chiral metal complexes not only have unique spatial configuration, various charges, different flexibilities, and hydrogen-bonding sites, but can also induce a chiral environment for the host framework.<sup>[9,10]</sup> Therefore, in search of novel organic-containing NCS thiometalates, our approach is to integrate non-centrosymmetric coordination polyhedra of Sb<sup>3+</sup> or As<sup>3+</sup> with metal tetrahedra (M = Ge, Ga, In, Hg, Sn, etc.) to form novel secondary building units (SBUs) in one structure in the presence of various [M(amine)<sub>m</sub>]<sup>n+</sup> (M = transition metal) cations or organic amines.<sup>[11–13]</sup> Such an approach has resulted in various thioantimonates with diverse architectures, and some of them are non-centrosymmetric or even chiral structures. Nevertheless, there is little progress on the preparation of chalcoarsenates and chalcoantimonates combining the In<sup>3+</sup> ion.<sup>[14–17]</sup> In particular, no polar indium thioantimonate has been isolated to date. Herein, we report the first polar indium thioantimonate, namely [Ni(en)<sub>3</sub>][InSbS<sub>4</sub>] (**1**) (en = ethylenediamine), with trinuclear heterometallic clusters of {In<sub>2</sub>SbS<sub>8</sub>} as secondary building units (SBU) and chiral [Ni(en)<sub>3</sub>]<sup>2+</sup> cations as the charge balancing agents.

## Results and Discussion

### Crystal Structure

Compound **1** was prepared from a mixture of In, Sb, S, and NiCl<sub>2</sub>·6H<sub>2</sub>O in ethylenediamine, which was sealed in a

[a] State Key Laboratory of Structural Chemistry, Fujian Institute of Research on the Structure of Matter, Chinese Academy of Sciences, Fuzhou, Fujian 350002, P.R. China  
Fax: +86-591-83793727  
E-mail: xyhuang@fjirsm.ac.cn

Supporting information for this article is available on the WWW under <http://dx.doi.org/10.1002/ejic.201100253>.

stainless steel reactor with a 28-mL Teflon liner, heated at 190 °C for 7 d. The product consisted of purple clubbed crystals of **1** and a small amount of unknown yellow powder. During the synthesis, the  $[\text{Ni}(\text{en})_3]^{2+}$  cation was formed in situ, which has been found in the syntheses of many thio-metalates.<sup>[18]</sup> Single-crystal X-ray crystallography<sup>[19]</sup> reveals that **1** belongs to the non-centrosymmetric space group  $R\bar{3}c$ . Its structure features a left-handed helical anionic chain of  $[\text{InSbS}_4]_n^{2n-}$  moieties built upon trinuclear heterometallic clusters of  $\{\text{In}_2\text{SbS}_8\}$  as SBUs. The asymmetric unit of **1** contains one crystallographically independent  $\text{In}^{3+}$  ion, one  $\text{Sb}^{3+}$  ion, one  $\text{Ni}^{2+}$  ion, four  $\text{S}^{2-}$  ions, and three ethylenediamine molecules (Figure S1). The  $\text{In}^{3+}$  ion is surrounded by four  $\text{S}^{2-}$  ions to form a tetrahedron, and the In–S bond lengths are 2.4503(10), 2.4528(9), 2.4590(9) and 2.4720(9) Å. The  $\text{Sb}^{3+}$  ion adopts a  $\{\text{SbS}_3\}$  trigonal-pyramidal coordination geometry with Sb–S bond lengths of 2.3625(9), 2.4292(10) and 2.4442(10) Å. The coordination geometry around the  $\text{Ni}^{2+}$  ion is a slightly distorted octahedron. In the  $[\text{Ni}(\text{en})_3]^{2+}$  cation, three chelating ethylenediamine molecules are coordinated to the  $\text{Ni}^{2+}$  ion to form a six-coordinate  $\text{Ni}^{2+}$  complex with  $\Lambda$  configuration in the examined single crystal of **1** (Figures 1a and S2).<sup>[9]</sup> The Ni–N bond lengths and N–Ni–N angles range from 2.091(3) to 2.151(3) Å and from 80.93(13) to 171.73(14)°, respectively. S(1) acts as a monodentate atom that is terminal, while S(2), S(3), and S(4) all act as bidentate metal linkers and bridge to one  $\text{In}^{3+}$  ion and one  $\text{Sb}^{3+}$  ion. Thus, two  $\{\text{InS}_4\}$  tetrahedra and one  $\{\text{SbS}_3\}$  trigonal pyramid share three corners to form a trinuclear heterometallic cluster with a stoichiometry of  $\{\text{In}_2\text{SbS}_8\}$  as the SBUs, in which there exists a six-membered ring of  $\{\text{In}_2\text{SbS}_3\}$  (Figure 1b). Similar  $\{\text{In}_2\text{SbS}_3\}$  rings have been observed in  $[\text{Ni}(\text{dien})_2]_3\cdot(\text{In}_3\text{Sb}_2\text{S}_9)_2\cdot 2\text{H}_2\text{O}$  and  $[\text{dpaH}]_5\text{In}_5\text{Sb}_6\text{S}_{19}\cdot 1.45\text{H}_2\text{O}$ ,<sup>[14,15]</sup> but both of them belong to different and more complex SBUs. The conformation of the  $\{\text{In}_2\text{SbS}_8\}$  SBU in **1** also is different from the pseudosemicycle with same composition in  $[\text{Ni}(\text{dien})_2]_2\text{In}_2\text{Sb}_4\text{S}_{11}$ <sup>[14]</sup> and the tetranuclear heterometallic SBUs of  $\{\text{Ga}_2\text{Sb}_2\text{S}_9\}$  in  $[\text{Ni}(\text{en})_3][\text{Ga}_2\text{Sb}_2\text{S}_7]$ <sup>[12]</sup> and  $\{\text{Sn}_2\text{Sb}_2\text{S}_{10}\}$  in  $[\text{La}(\text{en})_4\text{SbSnS}_5]_2\cdot 0.5\text{H}_2\text{O}$  (Figure S3).<sup>[13]</sup>

The  $\{\text{In}_2\text{SbS}_8\}$  SBUs are further interconnected by sharing  $\text{InS}_4$  tetrahedra to form a left-handed helical chain of  $[\text{InSbS}_4]_n^{2n-}$  running along the  $3_1$  axis parallel to the  $c$  axis in the examined single crystal of **1** (Figure 1c). One full turn of the left-handed helix contains four  $\text{InS}_4$  and three  $\text{SbS}_3$  polyhedra, with a pitch of 11.38 Å. The  $[\text{Ni}(\text{en})_3]^{2+}$  cations as the structure director and the charge balancing agent are located among the chains and form extensive N–H $\cdots$ S and C–H $\cdots$ S hydrogen bonds with the S atoms of the anionic chains (Figure S4), which results in a 3D supramolecular network, Figure 1d. The N–H $\cdots$ S and C–H $\cdots$ S hydrogen bond lengths and angles fall in the range 3.417(4)–3.730(4) Å and 133.2–169.6° (Table S2), respectively.

Although  $\text{Mn}(\text{tren})\text{InAsS}_4$  [ $\text{tren}$  = tris(2-aminoethyl)-amine] belongs to the space group  $P\bar{1}$  with a similar stoichiometry of the inorganic part,<sup>[17b]</sup> its structure is quite different from that of **1**.  $\text{Mn}(\text{tren})\text{InAsS}_4$  consists of a 1D inorganic  $[\text{InAsS}_4]_n^{2n-}$  chain constructed by the four-mem-

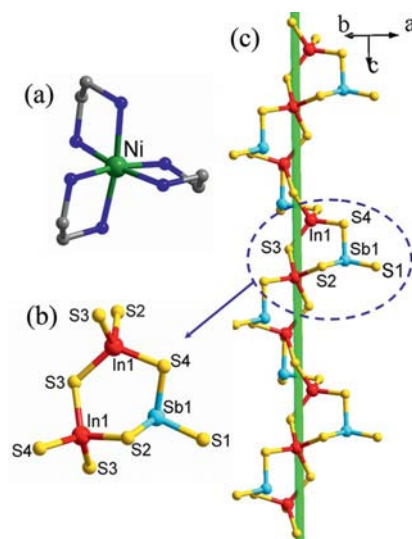


Figure 1. (a)  $[\text{Ni}(\text{en})_3]^{2+}$  with  $\Lambda$  configuration in the examined single crystal of **1**. Hydrogen atoms are omitted for clarity. (b) A section of the polymeric anion  $[\text{InSbS}_4]_n^{2n-}$  showing the trinuclear heterometallic cluster  $\{\text{In}_2\text{SbS}_8\}$  as the typical building unit in **1**. (c) A left-handed helical chain of  $[\text{InSbS}_4]_n^{2n-}$  running along the  $3_1$  axis parallel to the  $c$  axis in **1**.

bered  $\text{In}_2\text{S}_2$  ring and eight-membered  $\text{In}_2\text{As}_2\text{S}_4$  ring, and the  $[\text{Mn}(\text{tren})]^{2+}$  group directly bonds to the inorganic chain through Mn–S bonds (Figure S5), whereas the 1D inorganic  $[\text{InSbS}_4]_n^{2n-}$  chain in **1** is built upon the trinuclear heterometallic cluster  $\{\text{In}_2\text{SbS}_8\}$  and there are hydrogen-bonding interactions between the  $[\text{Ni}(\text{en})_3]^{2+}$  cation and the inorganic chain instead of Ni–S coordination bonds. Moreover, the 1D inorganic  $[\text{InSbS}_4]_n^{2n-}$  chain in **1** is helical, while the  $[\text{InAsS}_4]_n^{2n-}$  chain in  $\text{Mn}(\text{tren})\text{InAsS}_4$  is centrosymmetric. We also note that all known indium thioantimonates  $[\text{Ni}(\text{dien})_2]_2\text{In}_2\text{Sb}_4\text{S}_{11}$ ,  $[\text{Ni}(\text{dien})_2]_3(\text{In}_3\text{Sb}_2\text{S}_9)_2\cdot 2\text{H}_2\text{O}$ ,<sup>[14]</sup>  $[\text{dpaH}]_5\text{In}_5\text{Sb}_6\text{S}_{19}\cdot 1.45\text{H}_2\text{O}$ ,<sup>[15]</sup> and  $[\text{M}(\text{dap})_3]_3\text{InSb}_3\text{S}_7$  ( $\text{M} = \text{Co}, \text{Ni}$ )<sup>[16]</sup> belong to the centrosymmetric space groups. To the best of our knowledge, compound **1** is the first NCS indium thioantimonate (Figure 2).

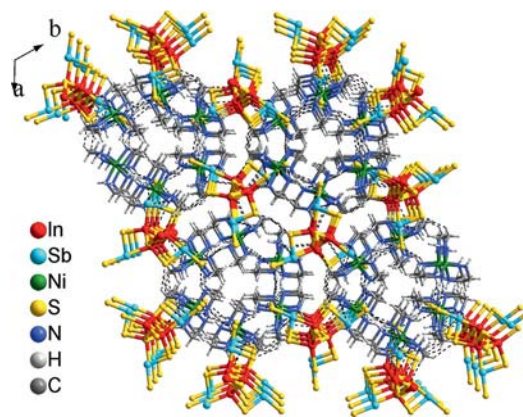


Figure 2. A perspective view of the 3D supramolecular network of **1** along the  $c$  axis formed by the H-bonding interaction between the inorganic anionic chains and the cations. Dotted lines show the extensive N–H $\cdots$ S and C–H $\cdots$ S hydrogen bonds in the structure.

## Optical Property

The optical absorption spectrum of **1** is plotted in Figure 3. The optical absorption edge of **1** is found to be 2.84 eV, close to that of the known indium thioantimonates such as  $[\text{Ni}(\text{dap})_3]\text{InSb}_3\text{S}_7$  (2.97 eV)<sup>[16]</sup> and  $[\text{Ni}(\text{dien})_2]_3\text{-(In}_3\text{Sb}_2\text{S}_9)_2\cdot 2\text{H}_2\text{O}$  (3.04 eV).<sup>[14]</sup> Relative to the bulk  $\text{In}_2\text{S}_3$  (2.3 eV) and  $\text{Sb}_2\text{S}_3$  (1.6 eV),<sup>[20]</sup> there is a noticeable blue shift of the absorption edge of **1**. In addition, the peaks at 1.47 and 2.28 eV in the absorption spectrum of **1** arise from a d–d electronic transition of the octahedrally coordinated  $\text{Ni}^{2+}$  ion in.

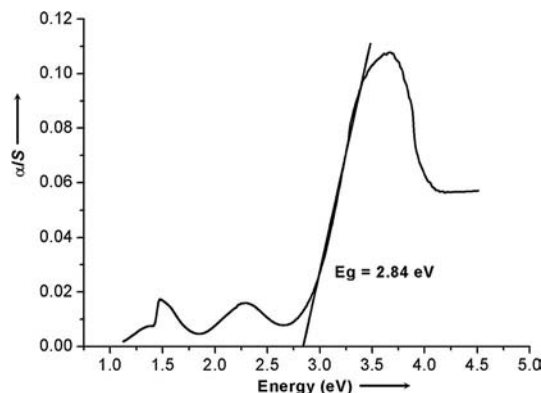


Figure 3. Solid-state optical absorption spectrum of **1**. The absorption spectrum was calculated from the diffuse reflectance spectrum by using the Kubelka–Munk function:  $a/S = (1 - R)^2/2R$ .<sup>[21]</sup>

## Thermal Stability Study

The thermal stability of **1** was examined on single-phase powder by thermogravimetric analysis (TGA) in a  $\text{N}_2$  atmosphere from 30 to 500 °C. The TG curve for **1** is shown in Figure S6 in the Supporting Information. It displays one main step, which corresponds to a weight loss of 30.6% from 200 to 300 °C. This indicates the loss of all the three en molecules per formula. The powder X-ray diffraction analyses of the TG residue indicate that the final residue is a mixture of  $\text{NiIn}_2\text{S}_4$  and  $\text{NiSbS}$  (Figure S7).

## Ferroelectric Property

Ferroelectricity strictly requires that the compound crystallizes in a non-centrosymmetric space group belonging to one of the ten polar point groups ( $C_1$ ,  $C_2$ ,  $C_s$ ,  $C_{2v}$ ,  $C_4$ ,  $C_{4v}$ ,  $C_3$ ,  $C_{3v}$ ,  $C_6$ ,  $C_{6v}$ ).<sup>[2]</sup> The space group  $R3c$  of **1** is associated with the point group  $C_{3v}$ . The experimental results indicate that compound **1** probably exhibits ferroelectric behavior. Figure 4 clearly shows that there is an electric hysteresis loop that is a typical ferroelectric feature with a remanent polarization ( $P_r$ ) of ca.  $0.021 \mu\text{C}/\text{cm}^2$  and coercive field ( $E_c$ ) of 7.2 kV/cm. The saturation spontaneous polarization ( $P_s$ ) of **1** is ca.  $0.029 \mu\text{C}/\text{cm}^2$ . The ferroelectric behavior indicates that the polarization is reversible. However, it is unlikely that the dipole moments associated with the non-centrosymmetric  $\text{SbS}_3$  trigonal pyramids are reversible, because

such reversal is energetically very unfavorable, as large structural rearrangements would be required. A similar phenomenon was observed in the other cations with lone-pair electrons such as  $\text{Se}^{4+}$ ,  $\text{Te}^{4+}$ ,  $\text{I}^{5+}$ .<sup>[5,22]</sup> Thus, the polarization reversibility is likely due to the small contribution from the  $\text{Ni}^{2+}$  cation. As a result, the macroscopic polarization coefficients are small in **1**.

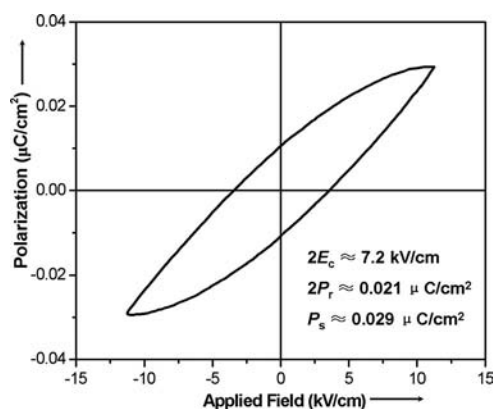


Figure 4. The electric hysteresis loop of **1**, observed for a powdered sample in the form of a pellet on a ferroelectric tester at the frequency of 2 Hz at room temperature.

## Theoretical Calculation

To gain further insight on the electronic structure of **1**, spin-polarized band structure as well as density of states (DOS) calculations for **1** based on the DFT method were made by using the total-energy code CASTEP.<sup>[23]</sup> The calculated band structure of **1** along high symmetry points of the first Brillouin zone is plotted in Figure S8. The state energies (eV) of the lowest conduction band (L-CB) and the highest valence band (H-VB) of **1** are listed in Table S3. The state energies (eV) of the lowest conduction band (1.44 eV) and the highest valence band (0.0 eV) are located at G point. Hence, the title compound has a direct band gap of around 1.44 eV. The calculated band gap is significantly smaller than the experimental value (2.84 eV). It is well known that the generalized gradient approximation does not accurately describe the eigenvalues of the electronic states, which often causes quantitative underestimation of band gaps for semiconductors and insulators.<sup>[24]</sup> The band can be assigned according to the total and partial DOS, as plotted in Figure 5. The CBs above the Fermi level (the Fermi level is set at 0.0 eV) are mainly derived from N-2p, Ni-3d, S-3p, Sb-5s, and Sb-5p states. The VBs from –8.57 eV to the Fermi level are mostly formed by C-2p, N-2p, Ni-3d, S-3p, Sb-5s, and Sb-5p states. The VBs between –16.6 and –8.57 eV are mainly composed of C-2s, C-2p, N-2p, S-3s, Sb-5s, and In-4d states and those from –22.5 to –18.2 eV are composed of N-2p and C-2s states and a small amount of the C-2p state.



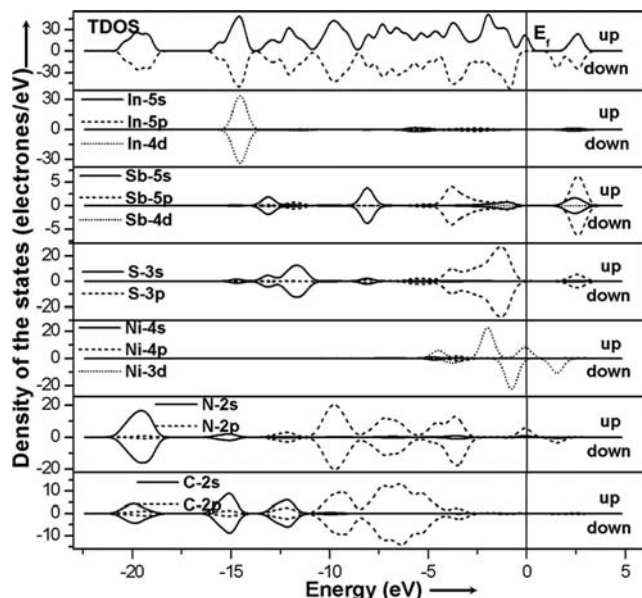


Figure 5. The total density of state and partial density of states for **1**. Fermi level is set at 0 eV.

## Conclusions

We have presented the solvothermal synthesis, crystal structure, thermal stability, optical and ferroelectric properties, as well as theoretical calculations of the first polar indium thioantimonate. It is interesting to combine the  $\text{InS}_4$  tetrahedron and the  $\text{SbS}_3$  non-centrosymmetric coordination geometry with chiral  $[\text{Ni}(\text{en})_3]^{2+}$  cation in a single crystal structure to form a NCS compound. The successful synthesis of **1** not only enriches the field of thiometalates but also provides a good example of NCS thiometalates with non-centrosymmetrical and chiral structural building units.

## Experimental Section

**Materials and Methods:** All chemicals employed in this study were of analytical grade and are commercially available, without the need for further purification. Elemental analyses of C, H, N and S were performed on a German Elementary Vario EL III instrument. The infrared spectrum was taken on a Magna 750 FTIR spectrometer with samples as KBr pellets in the range  $4000\text{--}400\text{ cm}^{-1}$ . Powder X-ray diffraction (PXRD) patterns were recorded on a Rigaku D/max 2500 diffractometer and a Rigaku MiniFlex II diffractometer by using  $\text{Cu-K}\alpha$  radiation. The optical diffuse reflectance spectrum was measured at room temperature with a Perkin-Elmer Lambda 900 UV/Vis spectrophotometer in the range  $200\text{--}1100\text{ nm}$ . A  $\text{BaSO}_4$  plate was used as a standard (100% reflectance). The absorption spectrum was calculated from reflectance spectra by using the Kubelka–Munk function:  $a/S = (1 - R)^2/2R$ ,<sup>[21]</sup> where  $a$  is the absorption coefficient,  $S$  the scattering coefficient, which is practically independent of wavelength when the particle size is larger than  $5\text{ }\mu\text{m}$ , and  $R$  the reflectance. Thermogravimetric analysis was carried out with a NETZSCH STA 449F3 unit at a heating rate of  $5\text{ }^\circ\text{C/min}$  under a nitrogen atmosphere. The measurement of the polarization–voltage curves was carried out on a pellet of the powder sample with an aixACCT TF Analyzer 2000 system at room temperature, the pellet (diameter of  $6\text{ mm}$  and

thickness of  $1\text{ mm}$ ) was sandwiched by silver electrodes and immersed in insulating oil during the measurement.

**Preparation of  $[\text{Ni}(\text{en})_3][\text{InSbS}_4]$  (**1**):** A mixture of Sb ( $0.0612\text{ g}$ ,  $0.50\text{ mmol}$ ), In ( $0.0545\text{ g}$ ,  $0.47\text{ mmol}$ ), S ( $0.1262\text{ g}$ ,  $3.94\text{ mmol}$ ), and  $\text{NiCl}_2\cdot 6\text{H}_2\text{O}$  ( $0.1193\text{ g}$ ,  $0.50\text{ mmol}$ ) in ethylenediamine ( $5\text{ mL}$ ) was sealed in a stainless steel reactor with a  $28\text{-mL}$  Teflon liner, heated at  $190\text{ }^\circ\text{C}$  for  $7\text{ d}$  and then cooled to room temperature. The product consisted of purple clubbed crystals of **1** and a very small amount of an unknown yellow powder. The crystalline products of **1** were selected by hand, washed by ethanol, and air dried (Yield:  $0.022\text{ g}$ ,  $8\%$  based on In).  $\text{C}_6\text{H}_{24}\text{In}_6\text{Ni}_6\text{S}_4\text{Sb}$  (**1**) ( $603.82$ ): calcd. C  $11.94$ , H  $4.01$ , N  $13.92$ , S  $21.24$ ; found C  $11.84$ , H  $3.87$ , N  $13.65$ , S  $20.74$ .

**Single-Crystal X-ray Crystallography:** The intensity data for **1** was collected on a Saturn70 CCD diffractometer with graphite-monochromated  $\text{Mo-K}\alpha$  radiation ( $\lambda = 0.71073\text{ \AA}$ ) at room temperature. The structure was solved by direct methods and refined by full-matrix least-squares on  $F^2$  by using the SHELX97 program package.<sup>[25]</sup> The hydrogen atoms attached to the C and N atoms in compound **1** are located at geometrically calculated positions. The empirical formula was confirmed by thermogravimetric analyses (TGA) and element analyses (EA). Selected bond lengths and angles of compound **1** are listed in Table S1, and selected hydrogen-bonding data of compound **1** are listed in Table S2. CCDC-808005 contains the supplementary crystallographic data of the crystal **1**. These data can be obtained free of charge from The Cambridge Crystallographic Data Centre via [www.ccdc.cam.ac.uk/data\\_request/cif](http://www.ccdc.cam.ac.uk/data_request/cif).

**Supporting Information** (see footnote on the first page of this article): Tables of bond lengths and angles, figures of the calculated band structure, IR spectra, TGA plots, and powder X-ray diffraction patterns.

## Acknowledgments

This work was supported by the Knowledge Innovation Program of the Chinese Academy of Sciences (KJXC2-XW-H21), the National Natural Science Foundation of China (NNSF of China) (Grants 20873149, 20803081), and the NSF of Fujian Province (No. 2008J0174, 2010J01056).

- [1] a) D. F. Eaton, *Science* **1991**, *253*, 281–287; b) J. F. Scott, *Science* **2007**, *315*, 954–959.
- [2] K. M. Ok, E. O. Chi, P. S. Halasyamani, *Chem. Soc. Rev.* **2006**, *35*, 710–717.
- [3] E. O. Chi, K. M. Ok, Y. Porter, P. S. Halasyamani, *Chem. Mater.* **2006**, *18*, 2070–2074.
- [4] a) F. Kong, S.-P. Huang, Z.-M. Sun, J.-G. Mao, W.-D. Cheng, *J. Am. Chem. Soc.* **2006**, *128*, 7750–7751; b) S.-P. Guo, G.-C. Guo, M.-S. Wang, J.-P. Zou, G. Xu, G.-J. Wang, X.-F. Long, J.-S. Huang, *Inorg. Chem.* **2009**, *48*, 7059–7065.
- [5] C.-F. Sun, C.-L. Hu, X. Xu, J.-B. Ling, T. Hu, F. Kong, X.-F. Long, J.-G. Mao, *J. Am. Chem. Soc.* **2009**, *131*, 9486–9487.
- [6] a) P. F. Bordui, M. M. Fejer, *Annu. Rev. Mater. Sci.* **1993**, *23*, 321–379; b) Y. Vysochanskii, *Ferroelectrics* **1998**, *218*, 629–636.
- [7] a) J. Zhou, J. Dai, G.-Q. Bian, C.-Y. Li, *Coord. Chem. Rev.* **2009**, *253*, 1221–1247; b) A. Kromm, T. van Almsick, W. S. Sheldrick, *Z. Naturforsch. B* **2010**, *65*, 918–936; c) B. Sedlhofer, N. Pienack, W. Bensch, *Z. Naturforsch. B* **2010**, *65*, 937–975.
- [8] a) T. K. Bera, J. H. Song, A. J. Freeman, J. I. Jang, J. B. Ketterson, M. G. Kanatzidis, *Angew. Chem.* **2008**, *120*, 7946–7950; *Angew. Chem. Int. Ed.* **2008**, *47*, 7828–7832; b) T. K. Bera, J. I.

- Jang, J. B. Ketterson, M. G. Kanatzidis, *J. Am. Chem. Soc.* **2009**, *131*, 75–77; c) Q. Zhang, I. Chung, J. I. Jang, J. B. Ketterson, M. G. Kanatzidis, *J. Am. Chem. Soc.* **2009**, *131*, 9896–9897.
- [9] Z.-E. Lin, J. Zhang, J.-T. Zhao, S.-T. Zheng, C.-Y. Pan, G.-M. Wang, G.-Y. Yang, *Angew. Chem.* **2005**, *117*, 7041–7044; *Angew. Chem. Int. Ed.* **2005**, *44*, 6881–6884.
- [10] Q.-C. Zhang, X. H. Bu, Z. Lin, M. Biasini, W. P. Beyermann, P. Y. Feng, *Inorg. Chem.* **2007**, *46*, 7262–7264.
- [11] a) M.-L. Feng, D.-N. Kong, Z.-L. Xie, X.-Y. Huang, *Angew. Chem.* **2008**, *120*, 8751–8754; *Angew. Chem. Int. Ed.* **2008**, *47*, 8623–8626; b) D.-N. Kong, Z.-L. Xie, M.-L. Feng, D. Ye, K.-Z. Du, J.-R. Li, X.-Y. Huang, *Cryst. Growth Des.* **2010**, *10*, 1364–1372; c) M.-L. Feng, W.-W. Xiong, D. Ye, J.-R. Li, X.-Y. Huang, *Chem. Asian J.* **2010**, *5*, 1817–1823.
- [12] M.-L. Feng, Z.-L. Xie, X.-Y. Huang, *Inorg. Chem.* **2009**, *48*, 3904–3906.
- [13] M.-L. Feng, D. Ye, X.-Y. Huang, *Inorg. Chem.* **2009**, *48*, 8060–8062.
- [14] J. Zhou, X.-H. Yin, F. Zhang, *Inorg. Chem.* **2010**, *49*, 9671–9676.
- [15] N. Ding, M. G. Kanatzidis, *Chem. Mater.* **2007**, *19*, 3867–3869.
- [16] J. Zhou, L. An, F. Zhang, *Inorg. Chem.* **2011**, *50*, 415–417.
- [17] a) D. M. Smith, M. A. Pell, J. A. Ibers, *Inorg. Chem.* **1998**, *37*, 2340–2343; b) Z. Wang, H. Zhang, C. Wang, *Inorg. Chem.* **2009**, *48*, 8180–8185; c) J.-H. Chou, M. G. Kanatzidis, *Inorg. Chem.* **1994**, *33*, 1001–1002.
- [18] a) H.-O. Stephan, M. G. Kanatzidis, *J. Am. Chem. Soc.* **1996**, *118*, 12226–12227; b) R. Stahler, B. D. Mosel, H. Eckert, W. Bensch, *Angew. Chem.* **2002**, *114*, 4671–4673; *Angew. Chem. Int. Ed.* **2002**, *41*, 4487–4489.
- [19] Crystal Data for **1**:  $\text{C}_6\text{H}_{24}\text{N}_6\text{InNiS}_4\text{Sb}$ ,  $M = 603.83$ , trigonal,  $R3c$ ,  $a = 29.3601(6)$ ,  $c = 11.3830(4)$  Å,  $V = 8497.7(4)$  Å<sup>3</sup>,  $Z = 18$ ,  $D_{\text{calcd.}} = 2.124$  g cm<sup>-3</sup>,  $F(000) = 5292$ ,  $\mu = 4.056$  mm<sup>-1</sup>,  $T = 293(2)$  K, 21517 reflections measured, 4250 unique reflections ( $R_{\text{int}} = 0.0399$ ), 4202 observed reflections [ $I > 2\sigma(I)$ ] with  $R1$  ( $wR2$ ) = 0.0208 (0.0440),  $R1$  ( $wR2$ ) = 0.0213 (0.0444) (all data),  $\text{GOF} = 1.050$ , abs. struc. 0.020(15).
- [20] a) T. Asikainen, M. Ritala, M. Leskela, *Applied Surface Science* **1994**, *82–3*, 122–125; b) T. Fujita, K. Kurita, K. Tokiyama, T. Oda, *J. Phys. Soc. Jpn.* **1987**, *56*, 3734–3739.
- [21] W. M. Wendlandt, H. G. Hecht, *Reflectance Spectroscopy*, Interscience, New York, **1966**.
- [22] a) R. E. Sykora, K. M. Ok, P. S. Halasyamani, T. E. Albrecht-Schmitt, *J. Am. Chem. Soc.* **2002**, *124*, 1951–1957; b) H. Y. Chang, S. H. Kim, P. S. Halasyamani, K. M. Ok, *J. Am. Chem. Soc.* **2009**, *131*, 2426–2427.
- [23] a) M. D. Segall, P. J. D. Lindan, M. J. Probert, C. J. Pickard, P. J. Hasnip, S. J. Clark, M. C. Payne, *J. Phys. Condens. Matter* **2002**, *14*, 2717–2744; b) V. Milman, B. Winkler, J. A. White, C. J. Pickard, M. C. Payne, E. V. Akhmatkaya, R. H. Nobes, *Int. J. Quantum Chem.* **2000**, *77*, 895–910.
- [24] a) R. W. Godby, M. Schluther, L. J. Sham, *Phys. Rev. B* **1987**, *36*, 6497–6500; b) C. M. I. Okoye, *J. Phys. Condens. Matter* **2003**, *15*, 5945–5958; c) R. Terki, G. Bertrand, H. Aourag, *Microelectron. Eng.* **2005**, *81*, 514–523.
- [25] G. M. Sheldrick, *SHELXS97 and SHELXL97*, University of Göttingen, Germany, **1997**.

Received: March 14, 2011

Published Online: May 19, 2011